25th ABCM International Congress of Mechanical Engineering
October 20-25, 2019, Uberlândia, MG, Brazil

COB-2019-0570
TRANSFERS BETWEEN COPLANAR CIRCULAR ORBITS AROUND EARTH WITH A LUNAR POWERED SWING-BY

Francisco Rebouças de Azevedo Júnior
Luiz Arthur Gagg Filho
Sandro da Silva Fernandes
Instituto Tecnológico de Aeronáutica, Praça Marechal Eduardo Gomes 50, Vila das Acácias, São José dos Campos, SP, Brasil
franciscojrns@gmail.com, arthurga@ita.br, sandro@ita.br

Abstract. *This work deals with the problem of transferring a spacecraft from a circular low Earth orbit (LEO) to a circular high Earth orbit (HEO) using a powered swing-by maneuver with the Moon. It is assumed that initial and final orbits are coplanar. A patched-conic approximation, based on the two-body dynamics, is used to describe the powered swing-by maneuver with the application of an intermediate impulse at the perilune. A Hohmann transfer between the elliptic orbit, which is described by the spacecraft after leaving the sphere of influence of the Moon, and the prescribed HEO is applied to complete the maneuver. Numerical simulations show that fuel saving can be obtained through such maneuver depending on the ratio between the radius of the initial and final orbits and the geometry of the swing-by, which is defined by a phase angle and the altitude of perilune.*

Keywords: *powered swing-by, transfers between circular orbits, patched-conic approximation, Hohmann transfers*

1. INTRODUCTION

The swing-by consists in a gravity-assisted space maneuver where a space vehicle uses gravitational influence of a massive celestial object, such as a planet or a star, to perform a change in trajectory without using any fuel. As discussed in Broucke (1988), these kind of maneuver are of much importance when performing interplanetary and cometary missions. The advantage of using the swing-by maneuver is tremendous, and, because of that, there are a large number of papers focusing on it. For exampĺe, Prado (1996) has utilized a patched-conic approximation to study the possibility of an intermediary impulse during the swing-by maneuver. Flandro (1966) has some interesting work regarding the determination of a favorable epoch to perform a swing-by with Jupiter in order to send a probe to outer planets. Despite the contributions of all the papers in the area, most of them considers the maneuver independently of the complete trajectory. Therefore, the present work shows an integrated analysis of the maneuver with the complete proposed trajectory.

2. OBJECTIVES

The present work intends to formulate a swing-by maneuver with an intermediate impulse in the context of the complete trajectory. It presents a preliminary analysis of the problem of transferring a space vehicle from a circular low Earth orbit (LEO) to a circular high Earth orbit (HEO) using a powered swing-by maneuver with the Moon. It is assumed that initial and final orbits are coplanar.

3. FORMULATION

The complete trajectory is split in two-phase: the first one is based on a patched-conic approximation, and, it is used to describe the powered swing-by maneuver with the application of an intermediate impulse at the perilune. The second phase is described by a Hohmann transfer between the elliptic orbits, and, it is described by the spacecraft after leaving the sphere of influence of the Moon, and the prescribed HEO. The geometry of the powered swing-by maneuver is defined by two main parameters: the phase angle between the spacecraft and the Moon at the entrance of the sphere of influence of the Moon, and, the altitude of the perilune.

3.1 Hohmann Transfer

The Hohmann maneuver is performed with the application of only two tangential impulses. The first one $\Delta\vec{v}_0$ is applied at the initial orbit, inserting the vehicle into an elliptical transfer trajectory. When it reaches the apogee of this trajectory, a second accelerative impulse $\Delta\vec{v}_f$ is applied so that the spacecraft enters into the prescribed final orbit.

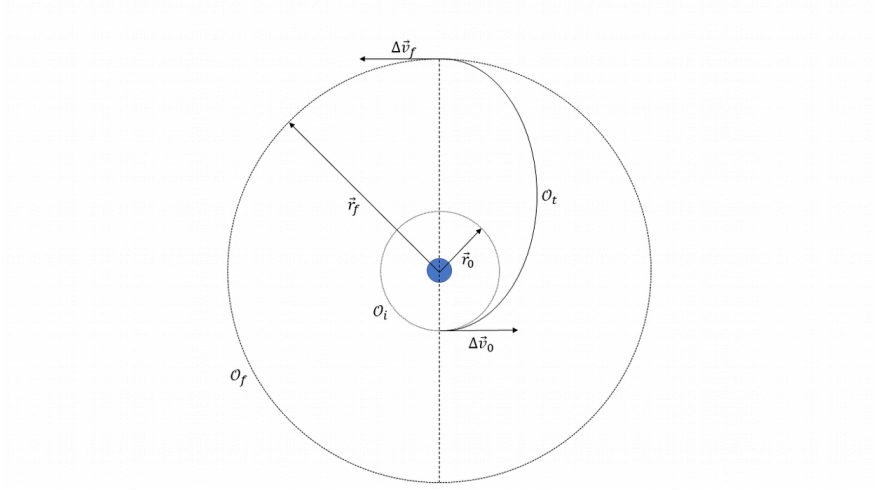

Figure 1: Hohmann Transfer.

This maneuver can be generalized when it is considered an elliptical final orbit instead of a circular one. In this case, the maneuver can be done in two different ways. The first one occurs when the orbit of destination has a perigee that is less than the radius of the initial orbit. In consequence, there is no intersection between the initial and final orbit. Nevertheless, if the final orbit has a perigee that is less than the radius of the departure orbit, both initial and final orbits intersects, and another situation is formed. Such configurations are presented in details in Fig. 2 and Fig. 3. The results using this variation of the problem is used in Section 4.3.

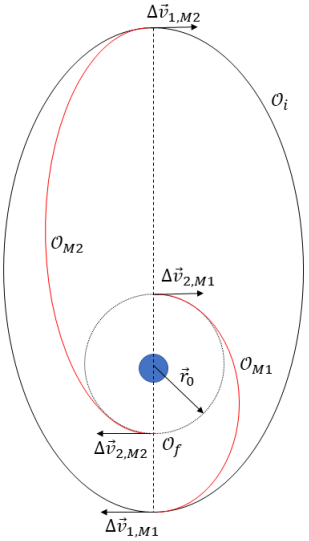

Figure 2: Generalized Hohmann transfer - mode 1.

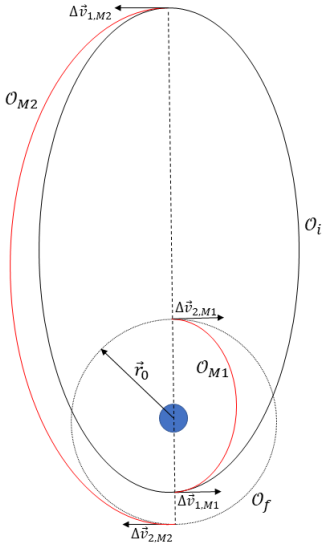

Figure 3: Generalized Hohmann transfer - mode 2.

3.2 Hoelker and Silber Transfer

The Holker and Silber transfer can be used to transfer a vehicle from a low Earth orbit (LEO) to a high Earth orbit (HEO), as shown in the Fig. 4.

Three instantaneous impulses are applied in this maneuver. They are applied tangentially to the considered orbits and in different points of the trajectory. The application of an intermediate impulse divides the transfer trajectory into two elliptical phases and that is why this maneuver is also known as the bi-elliptical.

3.3 Biparabolic Transfer

The Biparabolic Transfer shown in Fig. 5 is a purely theoretical transfer. It can be considered as a limiting case of the bi-elliptic transfer when r $\rightarrow \infty$. There are two applied finite impulses: the first one places the vehicle in the first parabolic orbit and the other inserts the vehicle in high orbit (HEO) when it comes from the second parabolic orbit. The transfer between the parabolic transfer orbits happens at an infinite distance with an infinitesimal impulse.

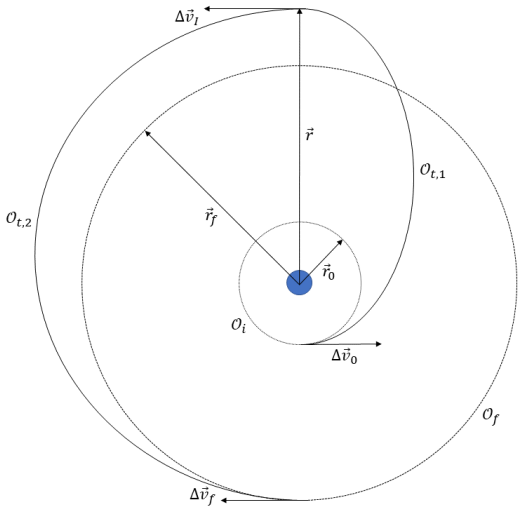

Figure 4: Holker and Silber Transfer Transfer.

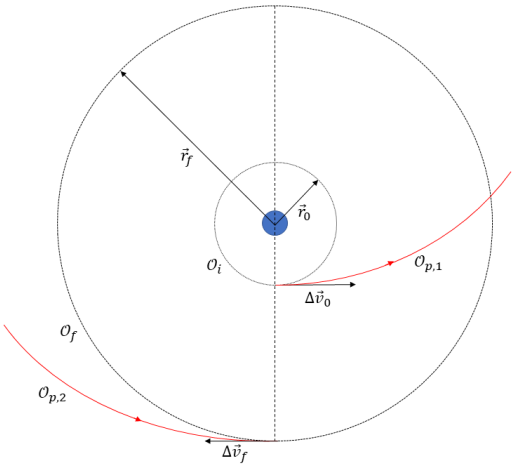

Figure 5: Biparabolic Transfer.

4. DESCRIPTION OF THE MANEUVER

The patched-conic approximation is a model based on the dynamics of the two-body problem and based on the concept of sphere of influence. It is employed in the preliminary calculation of a trajectory that transfers a spacecraft from a low Earth orbit (LEO) to a high Earth orbit (HEO), taking into account the gravitational attraction of the Moon in a swing-by maneuver. This Earth-Moon trajectory is obtained by the application of impulses at points of interest. The development of the patched-conic approximation for the natural or powered swing-by maneuver assumes the following hypothesis:

- The orbit of the Moon around the Earth is circular;
- The Earth is fixed in space;
- The vehicle remains at all times in the plane of motion of the Moon;
- Gravitational fields are central and obey Newton's law of gravitation;
- The impulses are applied tangentially to the initial and final orbits;
- The trajectory is divided into phases: two geocentric phases and one or two selenocentric phases, according to the type of swing-by - natural or powered. In each phase, the problem is solved considering only the attraction of the body with greater gravitational influence. In the geocentric phase, the Earth is considered as the attraction body, and, in the selenocentric, the Moon is considered.

4.1 First Geocentric Phase

According to Bate *et al.* (1971), four quantities define completely the first geocentric phase, as depicted in Fig. 4. These quantities are:

- Radius of the low Earth orbit (LEO), r_0;
- Magnitude of the velocity vector after application of the first impulse, v_0;

- Flight path angle at the injection point into the transfer trajectory of the first geocentric phase, φ_0;
- Phase angle that defines how the vehicle enters the sphere of influence of the Moon, λ_1.

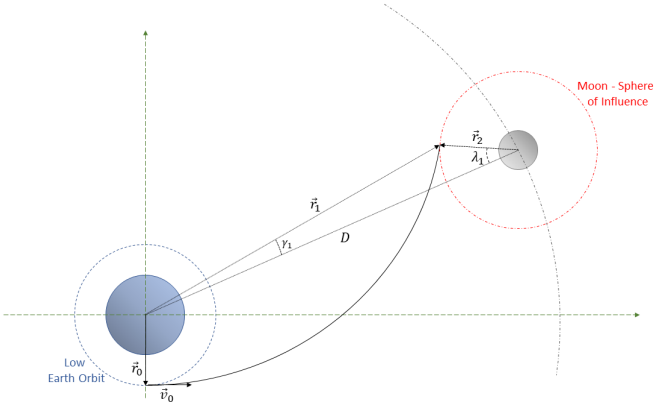

Figure 6: First geocentric phase description.

Once the initial parameters are specified, it is possible to calculate the characteristics of the trajectory corresponding to the first geocentric phase. Using the well-known solution of the two-body problem, one finds that the energy, ε, and the angular momentum, h, are expressed by:

$$\varepsilon = \frac{1}{2}v_0^2 - \frac{\mu_T}{r_0} \tag{1}$$

$$h = r_0 v_0 \cos\varphi_0 \tag{2}$$

where μ_T is the Earth's gravitational parameter.

The spacecraft travels along this path until the moment of contact with the sphere of influence of the Moon. The quantities at this point are denoted with subscript 1. From the geometry shown in Fig. 4 and conservation laws, the distance between the center of Earth and the contact at the SoI, r_1, the velocity at that point, v_1, and the flight path angle, φ_1, can be found Gagg Filho and Fernandes (2016):

$$r_1 = \sqrt{D^2 + r_2^2 - 2Dr_2\cos\lambda_1} \tag{3}$$

$$\sin\gamma_1 = r_2\frac{\sin\lambda_1}{r_1} \tag{4}$$

$$v_1 = \sqrt{2\left(\varepsilon + \frac{\mu_T}{r_1}\right)} \tag{5}$$

$$\cos\varphi_1 = \frac{h}{r_1 v_1} \tag{6}$$

where D is the distance between the center of the Earth and the center of the Moon, r_2 is the radius of the sphere of influence of the Moon, and, γ_1 is a phase angle between the spacecraft and the Moon.

The eccentric anomaly E_1 can be determined without ambiguity since the contact of the vehicle with the sphere of influence of the Moon occurs before the apogee of the trajectory described in this first geocentric phase, and, it is given by:

$$\cos E_1 = \frac{1}{e_0}\left(1 - \frac{r_1}{a_0}\right) \tag{7}$$

where a_0 e e_0 are, respectively, the semi-major axis and the eccentricity of the transfer orbits, expressed by:

$$e_0 = \sqrt{1 + Q_0(Q_0 - 2)} \tag{8}$$

$$a_0 = \frac{r_0}{2 - Q_0} \tag{9}$$

where $Q_0 = r_0 v_0^2/\mu_T$.

In order to complete the characterization of this phase, it is necessary to calculate its duration time. For this, the equation of flight time for elliptical orbits is used: the Kepler equation. The expression for the flight time Δt_{GEO} of the first geocentric phase is given by:

$$\Delta t_{GEO} = \sqrt{\frac{a_0^3}{\mu_T}}(E_1 - e_0 \sin E_1) \tag{10}$$

4.2 Selenocentric Phase

The swing-by maneuver corresponds to the selenocentric phase of the trajectory. In the natural swing-by maneuver, the trajectory is defined by only one hyperbole. In the powered swing-by, the trajectory is defined by two distinct hyperboles with a common perilune. The selenocentric phase is shown in detail in Fig. 7 for both swing-by maneuvers, where N denotes the natural swing-by, and, P denotes the powered swing-by.

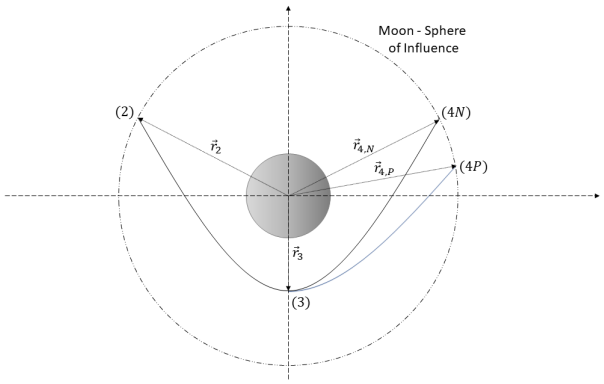

Figure 7: Selenocentric phase description.

4.2.1 Approximation Trajectory

At the contact point with the sphere of influence of the Moon, it is necessary to calculate some quantities with respect to the Moon. The subscript 2 is used to denote the new quantities.

Noting that $\vec{v}_2 = \vec{v}_1 - \vec{v}_L$, it is possible to calculate the magnitude of the velocity, v_2, and the flight path angle, φ_2, at that point:

$$v_2 = \sqrt{v_1^2 + v_L^2 - 2 v_1 v_L \cos(\varphi_1 - \gamma_1)} \tag{11}$$

$$\tan(\lambda_1 \pm \varphi_2) = \frac{-v_1 \sin(\varphi_1 - \gamma_1)}{v_L - v_1 \cos(\varphi_1 - \gamma_1)} \tag{12}$$

where v_L denotes the magnitude of the velocity vector of the Moon in its circular orbit;

The angle φ_2 is the flight path angle at the beginning of the selenocentric phase. The upper sign is chosen for a clockwise path, and, the lower sign is for a counterclockwise one. From these quantities, the trajectory can be characterized, calculating its semi-major axis, a_2, and its eccentricity, e_2:

$$a_2 = \frac{r_2}{2 - Q_2} \tag{13}$$

$$e_2 = \sqrt{1 + Q_2(Q_2 - 2)\cos^2 \varphi_2} \tag{14}$$

where $Q_2 = r_2 v_2^2/\mu_L$ and μ_L is the gravitational parameter of the Moon.

The closest distance of the vehicle with respect the Moon, r_{SB}, also called perilune, is calculated from:

$$r_{SB} = a_2(1 - e_2) \tag{15}$$

If the distance r_{SB} found is equal to the prescribed value, then the first impulse is the correct one. However, it may happen that the perilune does not match the desired one. In this case, the first impulse must be adjusted to satisfy the prescribed value of r_{SB} by means of an iterative procedure. In this work, Newton-Raphson method is applied to solve such intermediate value problem.

4.2.2 Escape Trajectory - Powered Swing-by

The velocity at the perilune of the selenocentric trajectory before the application of the impulse is given by:

$$v = \sqrt{\frac{\mu_L(1+e_2)}{a_2(1-e_2)}} \tag{16}$$

Denoting the applied impulse by Δv_i, the new velocity resulting from this increment is:

$$v_p = v + \Delta v_i \tag{17}$$

While there is a change in the velocity, the perilune of the trajectory is not changed, since the impulse is applied tangentially to the orbit. Since the flight path angle φ_3 is null, one can then determine the value of the semi-major axis, a_p and the eccentricity, e_p, of the new orbit through the following expressions:

$$a_p = \frac{r_2}{2 - Q_p} \tag{18}$$

$$e_p = \sqrt{1 + Q_p(Q_p - 2)\cos^2\varphi_3} \tag{19}$$

where $Q_p = r_2 v_p^2/\mu_L$.

With the above results, the trajectory that is described by the vehicle after the application of the intermediate impulse is determined. In order to calculate the quantities relevant to the characterization of the orbit in the second geocentric phase, it is necessary to calculate some properties of the orbit at the point of exit from the sphere of influence, still in relation to the Moon. Using conservation of energy and conservation of angular momentum, one can determine the velocity, v_4, and the flight path angle φ_4:

$$v_4 = \sqrt{v_p^2 + 2\mu_L\left(\frac{1}{r_2} - \frac{1}{r_{SB}}\right)} \tag{20}$$

$$\cos\varphi_4 = \frac{r_{SB} v_p}{r_2 v_4} \tag{21}$$

4.3 Second Geocentric Phase

The second geocentric phase begins exactly when the vehicle leaves the sphere of influence of the Moon. At that moment, the gravity of the Moon is no longer considered and only the Earth has influence on the spacecraft. In this way, it is necessary that the quantities be recalculated in relation to the fixed system that is the Earth itself. A second velocity composition is needed by noting that $\vec{v}_5 = \vec{v}_4 + \vec{v}_L$. Subscript 5 now indicates that the magnitudes of point 4 are being calculated relative to Earth. Thus, the distance between the spacecraft and the center of the Earth, r_5, the new phase angle between the spacecraft and the Moon, γ_4, the velocity at that point, v_5, and finally, the flight path angle φ_5 can be calculated:

$$r_5 = \sqrt{D^2 + r_4^2 - 2Dr_4\cos\lambda_4} \tag{22}$$

$$\sin\gamma_4 = r_4\frac{\sin\lambda_4}{r_5} \tag{23}$$

$$v_5 = \sqrt{v_4^2 + v_L^2 - 2v_4 v_L\cos(\lambda_4 + \varphi_4)} \tag{24}$$

$$\tan(\varphi_5 - \gamma_4) = \frac{-v_4\sin(\lambda_4 + \varphi_4)}{v_L - v_1\cos(\lambda_4 + \varphi_4)} \tag{25}$$

The trajectory in the second geocentric phase is determined through the parameters calculated from Eqs. (22), (23), (24) and (25). During this phase, the maneuver can be performed in two ways. In the first, the impulse to insert the spacecraft into the transfer orbit is applied at the perigee, while in the second the impulse is applied at the apogee. Figures 8 and 9 show in detail how these situations can occur.

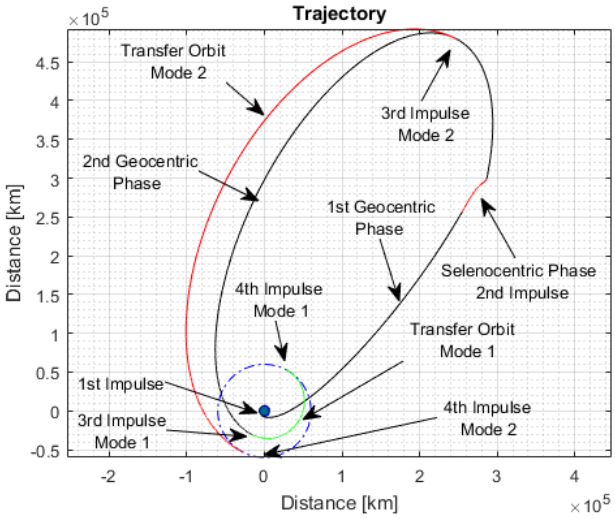

Figure 8: Transfer without intersection between the orbits.

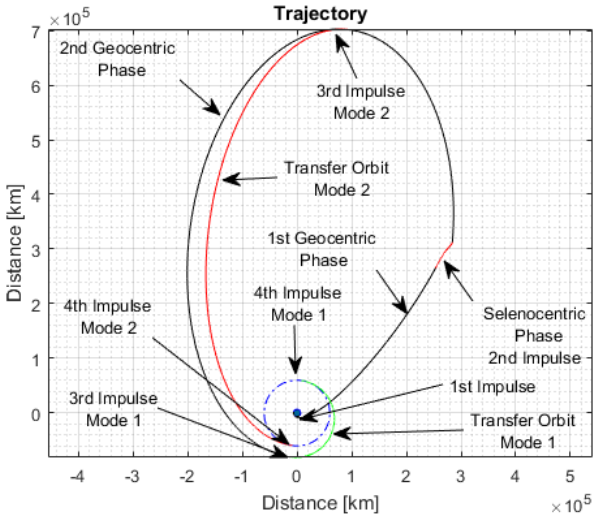

Figure 9: Transfer with intersection between the orbits.

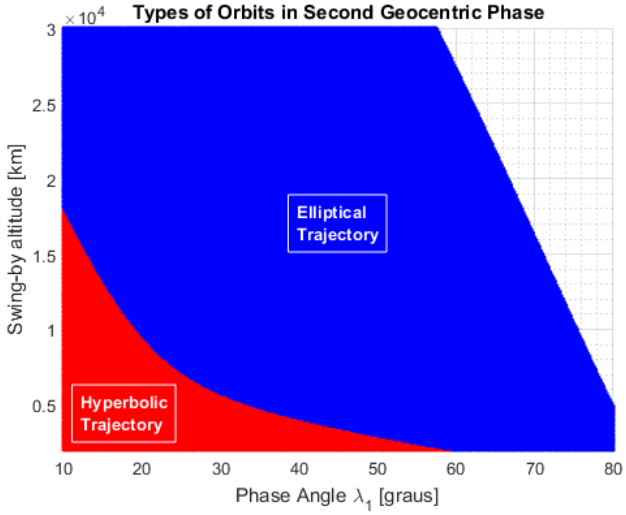

Figure 10: Types of Orbits in Second Geocentric Phase.

5. RESULTS

The results that are shown here refer to a circular low Earth orbit with altitude of 167 km. The swing-by is performed in the counterclockwise direction. First, a routine is used to check what types of orbits are obtained as the swing-by altitude h_{SB} and the phase angle λ_1 are increased. For the swing-by altitude, a range of 2000 km up to 30000 km is used. For the phase angle λ_1, the range is 10 degrees to 80 degrees. The results, also found by Gagg Filho and Fernandes (2016), are shown in Fig. (10).

It can be seen that hyperbolic orbits, most often used for interplanetary trajectories, are obtained by using low phase angle and swing-by altitude values closer to the lunar surface. The elliptic trajectories, which are used to return the spacecraft to high Earth orbit (HEO), are found in most combinations (λ_1, r_{SB}). For high values of phase angle and swing-by altitude, the algorithm does not converge. Note that the orbits concerning to the second geocentric phase in Fig. 8 are found using natural swing-by. If accelerative impulses occur, more hyperbolic trajectories arise in the figure, since the orbit becomes more energetic. The opposite occurs if the spacecraft is decelerated: more elliptical orbits arise during the second geocentric phase.

Once determined how the types of orbits of the second geocentric phase behave by varying the phase angle and the swing-by altitude, it is studied how eccentricity, semi-major axis, apogee and perigee of these orbits behave when the altitude of swing-by and the boost in the perilune are prescribed.

Figures 11 and 12 represent the eccentricity and the perigee radius as functions of the phase angle λ_1 for several values of Δv_i, considering accelerative and decelerative impulses. Dashed curves represent the orbits found when accelerative impulses are applied at the closest point to the Moon, and, the solid curves represent the orbits obtained using decelerative impulses. The orbits are calculated for swing-by altitudes of 10000 km and 20000 km.

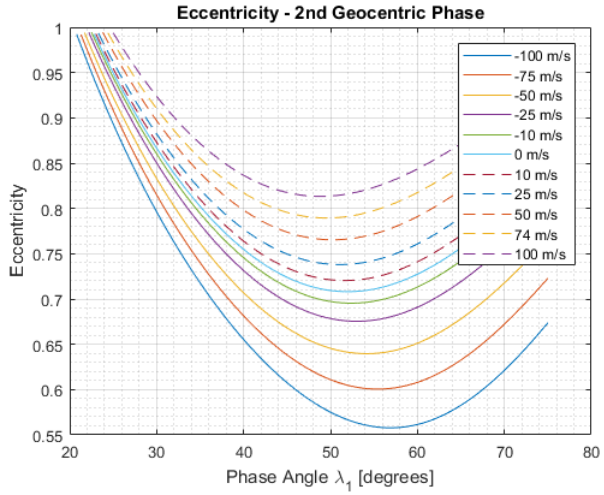

Figure 11: Eccentricity [$h_{SB} = 10000$ km].

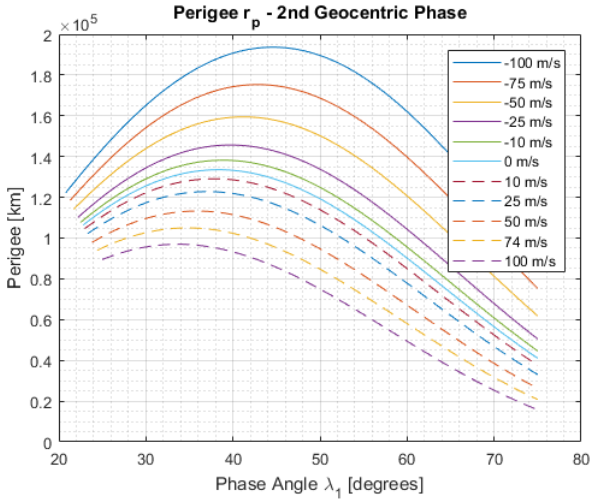

Figure 12: Perigee [$h_{SB} = 10000$ km].

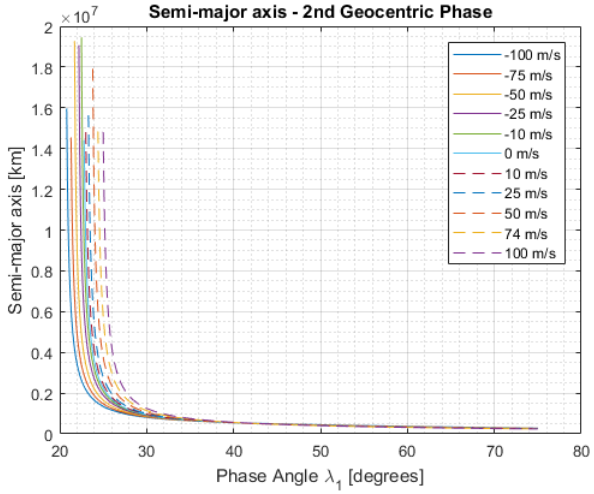

Figure 13: Semi-major axis [$h_{SB} = 10000$ km].

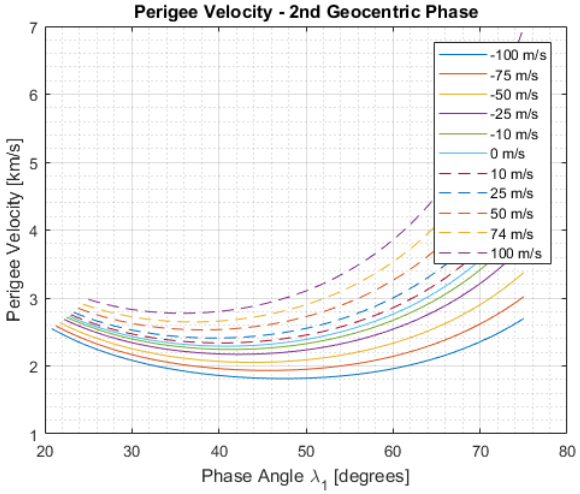

Figure 14: Perigee velocity [$h_{SB} = 10000$ km].

According to the Fig. (11), lower swing-by altitudes lead to more eccentric orbits for small-phase angles, and, accelerative impulses lead to considerably more eccentric orbits, while decelerating impulses lead to less eccentric orbits.

Figure (12) shows that the closer the swing-by, the smaller is the perigee of the second geocentric phase, and, therefore, the closer the vehicle pass from Earth on its way back. Accelerative impulse also brings the perigee closer to Earth.

Note that although there are situations where the perigee radius of the second geocentric phase is relatively low, the velocities in the perigee are very high. This fact compromises the use of a LEO-HEO maneuver. High velocities at the perigee of these orbits, which are quite eccentric, make the decelerating impulse to circularize very high and therefore, it makes a mission unfeasible.

With these results on the behavior of the parameters of the elliptic orbits of the second geocentric phase, it is now possible to analyze the problem of transferring the vehicle from a circular low Earth orbit (LEO) to a circular high Earth orbit (HEO) taking as an intermediate transfer orbit some of those orbits found on exit of the SoI of the Moon.

In the search for a transfer that provides the lowest fuel consumption, the increments found by the proposed maneuver with the swing-by with the Moon are compared with the increments required to perform the same maneuver using the well-known Hohmann and Biparabolic transfers previously described in Section 2.

By comparing with the Hohmann maneuver; it is possible to confirm some expected behavior. For mode 1 transfer, for example, the Fig. (15) shows a need for a larger boost to perform the complete maneuver, precisely because it is a transfer that occurs closer to Earth and therefore more energetic.

There are orbits that can be reached via a lunar swing-by whose total velocity increment is smaller than a direct transfer using the Hohmann or biparabolic maneuver. It should be noted that there must be a minimum ΔV_T, which is the total velocity increment for a specific λ_1. By formulating this optimization problem, it will be possible to determine the most economical trajectory in terms of velocity increment in relation to Hohmann and biparabolic transfers.

Tables 1-6 show the following parameters: λ_1, ΔV_T, the difference between the total velocity increment and the

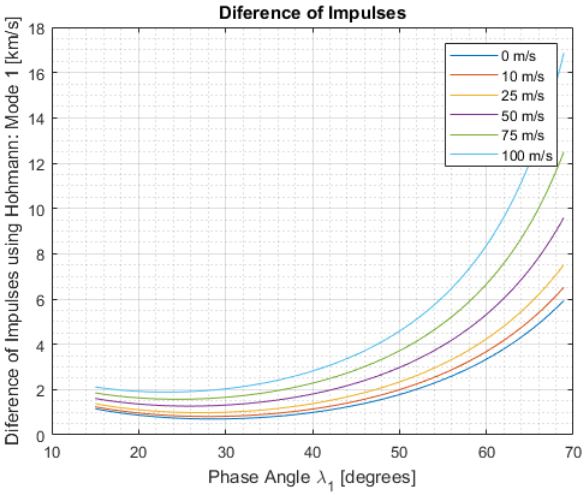

Figure 15: Comparison between Hohmann transfer and mode 1 transfer [$h_{SB} = 20000$ km, $h_{HEO} = 80000$ km].

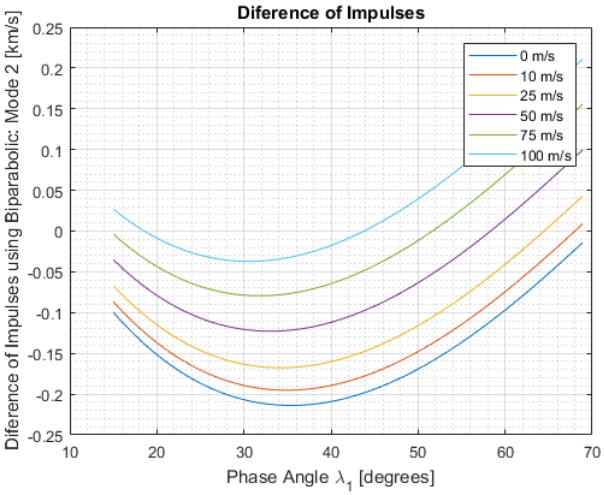

Figure 16: Comparison between Biparabolic transfer and mode 2 transfer [$h_{SB} = 20000$ km, $h_{HEO} = 80000$ km].

velocity increment obtained using the Hohmann transfer ΔV_{T-H}, and, the difference between the total velocity increment and the velocity increment using the biparabolic tranfer ΔV_{T-BP}. Each table refers to a specific distance of maximum approximation to the surface of the Moon r_{SB} and a radius of the high Earth orbit. Note that there exist transfers with lunar swing-by, powered or not, that are more economic than Hohmann or biparabolic transfers.

Table 1: $r_{SB} = 10000$ km and $h_{HEO} = 40000$ km.

Mode	λ_1 [degree]	ΔV_T [km/s]	ΔV_{T-H} [km/s]	ΔV_{R-BP} [km/s]
1	30	5.119	1.210	0.579
1	40	5.056	1.146	0.516
1	50	4.987	1.078	0.447
1	60	4.886	0.976	0.346
2	30	4.519	0.609	-0.020
2	40	4.534	0.625	-0.005
2	50	4.527	0.617	-0.012
2	60	4.481	0.571	-0.058

Table 2: $r_{SB} = 20000$ km and $h_{HEO} = 60000$ km.

Mode	λ_1 [degree]	ΔV_T [km/s]	ΔV_{T-H} [km/s]	ΔV_{R-BP} [km/s]
1	30	4.290	0.180	-0.009
1	40	4.485	0.375	0.185
1	50	5.119	1.009	0.819
1	60	6.404	2.294	2.104
2	30	4.071	-0.038	-0.229
2	40	4.058	-0.051	-0.241
2	50	4.091	-0.018	-0.208
2	60	4.158	0.048	-0.141

Table 3: $r_{SB} = 10000$ km and $h_{HEO} = 60000$ km.

Mode	λ_1 [degree]	ΔV_T [km/s]	ΔV_{T-H} [km/s]	ΔV_{R-BP} [km/s]
1	30	4.624	0.514	0.324
1	40	4.571	0.461	0.271
1	50	4.491	0.381	0.191
1	60	4.358	0.249	0.058
2	30	4.245	0.135	-0.054
2	40	4.236	0.126	-0.063
2	50	4.210	0.100	-0.089
2	60	4.150	0.040	-0.149

Table 4: $r_{SB} = 10000$ km and $h_{HEO} = 80000$ km.

Mode	λ_1 [degree]	ΔV_T [km/s]	ΔV_{T-H} [km/s]	ΔV_{R-BP} [km/s]
1	30	4.303	0.132	0.146
1	40	4.255	0.084	0.098
1	50	4.170	-0.0004	0.013
1	60	4.024	-0.146	-0.132
2	30	4.073	-0.097	-0.083
2	40	4.045	-0.125	-0.111
2	50	4.006	-0.164	-0.150
2	60	3.935	-0.235	-0.221

Table 5: $r_{SB} = 20000$ km and $h_{HEO} = 40000$ km.

Mode	λ_1 [degree]	ΔV_T [km/s]	ΔV_{T-H} [km/s]	ΔV_{R-BP} [km/s]
1	30	4.543	0.633	0.002
1	40	4.431	0.521	-0.108
1	50	4.502	0.592	-0.037
1	60	5.747	1.837	1.207
2	30	4.364	0.454	-0.175
2	40	4.320	0.410	-0.219
2	50	4.288	0.378	-0.251
2	60	4.352	0.442	-0.187

Table 6: $r_{SB} = 20000$ km and $h_{HEO} = 80000$ km.

Mode	λ_1 [degree]	ΔV_T [km/s]	ΔV_{T-H} [km/s]	ΔV_{R-BP} [km/s]
1	30	4.656	0.485	0.499
1	40	4.859	0.688	0.702
1	50	5.507	1.336	1.350
1	60	6.803	2.632	2.646
2	30	3.956	-0.214	-0.200
2	40	3.948	-0.222	-0.208
2	50	3.983	-0.187	-0.173
2	60	4.053	-0.117	-0.103

6. CONCLUSIONS

Finding ways to cheapen space missions will always be a priority for those who aim to make this kind of knowledge more accessible. This work has been conceived for this purpose: to present possibilities of trajectory that provide a lower fuel consumption than those calculated by the traditional methods. According to the results presented, it is verified that, for certain combinations of h_{SB}, λ_1 and Δv_i, the model described by the patched-conic approximation together with the possibility of the application of an impulse in perilune, lead to better results that those obtained by other types of maneuvers. It is valid, however, to emphasize that the Hohmann maneuver still appears as the best option for transfers occurring between orbits that are closer together.

The model presented here in a simplified way, that uses the results for the two-body problem, can be taken to a more complete study involving the three, four and five-body problems. Then, a more general and closer picture of the reality can be obtained and used to find more accurate data about fuel consumption in those missions.

One can consider the hyperbolic orbits that are obtained at the exit from the sphere of influence of the Moon to study interplanetary maneuvers. In these missions, one possibility is to choose a planet, such as Venus or Mars, in order to study the fuel consumption to put the vehicle in an orbit around these planets. As a complement, an optimization algorithm can be implemented to search for a minimum fuel consumption orbit.

7. REFERENCES

Bate, R.R., Mueller, D.D. and White, J.E., 1971. *Fundamentals of astrodynamics*. Courier Corporation.

Broucke, R., 1988. "The celestial mechanics of gravity assist". *AIAA/AAS ASTRODYNAMICS CONFERENCE*, pp. 69–78.

Flandro, G., 1966. "Fast reconnaissance missions to the outer solar system utilizing energy derived from the gravitational field of jupiter". *Astronautica Acta*, Vol. 12, pp. 329–337.

Gagg Filho, L.A. and Fernandes, S.S., 2016. "Aproximação patched-conic lunar com manobra de swing-by". *Congresso Nacional de Engenharia Mecânica*.

Jones, D.R., 2016a. "Trajectories for europa flyby sample return". *AIAA/AAS ASTRODYNAMICS CONFERENCE*.

Jones, D.R., 2016b. "Trajectories for flyby sample return at saturn's moons". *AIAA/AAS ASTRODYNAMICS CONFERENCE*.

Prado, A.F.B.A., 1996. "Powered swing-by". *Journal of Guidance, Control and Dynamics*, Vol. 19, pp. 1142–1147.

8. RESPONSIBILITY NOTICE

The authors are the only responsible for the printed material included in this paper.